ADVANCED MATERIALS INTERFACES
Open Access
www.advmatinterfaces.de

Designer Adhesives for Tough and Durable Interfaces in High-Performance Ti-Carbon PEKK Hybrid Joints

Georgios Kafkopoulos, Vanessa M. Marinosci, Joost Duvigneau, Wouter J. B. Grouve, Sebastiaan Wijskamp, Matthijn B. deRooij, G. Julius Vancso, and Remko Akkerman**

Advanced high-performance structural applications require the right materials in the right place and suitable interface engineering. However, poor adhesion in harsh environmental conditions frequently challenge material interfaces. An example is the moisture sensitivity of titanium-poly ether ketone ketone (PEKK) interfaces. Here, this work offers a high-performance composite adhesive system, which combines strong adhesion and high interfacial toughness, particularly when used in metal-polymer bonding. This system includes aminopropyl triethoxy silane (APTES)–polydopamine (SiPDA) layers, which can be formed on the titanium surface before the joining process with carbon fiber-reinforced PEKK (C/PEKK). Adhesion between PEKK and titanium is evaluated before and after hot/wet conditioning using mandrel peel tests. This work discovers that applying thin SiPDA layers not only results in a remarkable rise in the interfacial fracture toughness but also provides durable bond stability after hot/wet conditioning. These findings indicate that polydopamine-based coatings show great potential to achieve stable interfaces for the next generation of high-performance metal-polymer hybrid materials.

1. Introduction

Having the right materials in the right place is key for high-performance, lightweight structures in load-bearing applications.[1,2] This requirement often entails hybridization, meaning that high-performance materials from different classes are combined, resulting in hybrid materials characterized by superior properties compared to the properties of the individual constituents.[3] The combination of high-performance polymer composites with metals is a representative example. The transportation industry often uses this material combination since metal inserts in composite structures enable efficient load transfer between components of the composite assembly.[4] Another example of a hybrid metal-composite structure includes Fiber Metal Laminates (FMLs), which are particularly suitable for aerospace applications as they combine high specific stiffness and strength with high impact and fatigue resistance.[5]

Implementing thermoplastic composites (TPCs) in hybrid materials brings further advantages, such as a higher toughness and lower flammability than their unfilled thermoset counterparts.[6] Additionally, the melt-processability of the thermoplastic matrix allows TPC parts to be manufactured using short processing times[7] and to be joined by welding[8] or co-consolidation.[9] Therefore, the use of TPCs in hybrid assemblies can be beneficial also from a manufacturing perspective, as these joining methods typically save time and costs compared to standard joining technologies like mechanical fastening or adhesive bonding.[10]

Nowadays, typical TPCs employed in aerospace are made of high-performance thermoplastic matrices such as PEEK or PEKK in combination with continuous carbon fibers.[11] However, joining a carbon fiber-based composite with traditional metals like aluminium or steel may induce galvanic corrosion of the metal part.[12] Using titanium alloys allows to avoid any risk of corrosion, due to the galvanic compatibility between titanium and graphite. As a consequence, in terms of material system, titanium alloys are often used in combination with both thermoplastic and thermoset-based composites with carbon fibers.

An example of aerospace application in which titanium is combined to TPCs is in FML systems. There has been an increased interest in FMLs based on titanium, also called hybrid titanium composite laminates (HTCLs), as using titanium instead of aluminium further improves the mechanical properties at both room and elevated temperatures.[5] Additionally, using TPCs in the HTCLs further enhances toughness and impact resistance of the resulting hybrid material.[13] A direct consequence of this material hybridization is the formation

G. Kafkopoulos, J. Duvigneau, G. J. Vancso
Department of Materials Science and Technology (MTP) of Polymers and Sustainable Polymer Chemistry (SPC)
University of Twente
Enschede 7522 NB, The Netherlands
E-mail: g.j.vancso@utwente.nl

V. M. Marinosci, S. Wijskamp, R. Akkerman
ThermoPlastic composites Research Center (TPRC)
Palatijn, Enschede 15 7521PN, The Netherlands
E-mail: r.akkerman@utwente.nl

V. M. Marinosci, W. J. B. Grouve, M. B. Rooij, R. Akkerman
Department of Engineering Technology (ET)
University of Twente
Enschede 7522 NB, The Netherlands

The ORCID identification number(s) for the author(s) of this article can be found under https://doi.org/10.1002/admi.202202460.

DOI: 10.1002/admi.202202460

of interfaces whose mechanical performance and durability are critical to the overall performance of the structure. Several studies demonstrated that metal surface modification before bonding through creating optimized mechanical interlocking[14] and/or molecular interactions[15] is fundamental to promoting adhesion between the two different adherents.

It has been pointed out that the adhesion stability of these types of interfaces is frequently challenged by environmental conditions such as humidity and/or elevated temperature.[16] Exposing the joints to such conditions often leads to severe deterioration of the interfacial bond. An example is the notorious adhesion instability in hot/humid environmental conditions between poly-aryl-ether-ketone (PAEK) polymers and metals like titanium[17] or steel.[12]

The root cause of the bond instability between titanium and PEKK in the presence of water has been recently reported for co-consolidated titanium-carbon/PEKK joint.[18] This report showed that the reversible nature of the molecular interaction and the tendency of native titanium oxide surfaces to adsorb water leads to significant decline of the mechanical performance when exposing the joints to a hot/humid environment.[18] There is only a limited number of surface treatments that improve the moisture resistance for this type of interfaces.[17,19,20] Thus, the present study aims at providing hot/wet conditioning resistance to titanium-C/PEKK joints by modifying the surface chemistry of the titanium surface before the joining process.

Polydopamine (PDA) has drawn increasing attention over the past years as a surface modification technique. PDA was first introduced by Messersmith and co-workers,[21] by inducing the oxidative polymerization of dopamine in basic conditions. During the polymerization process of PDA, a thin film is formed on the surface of virtually any object immersed in the polymerization solution.[21] The extraordinary versatility of PDA in terms of molecular interactions in combination with the strong adhesion promoted by catechol moieties present in PDA render these coatings an attractive option for promoting adhesion at thermoplastic polymer/metal interfaces.[22]

PDA-based coatings with titanium oxide surfaces are quite interesting due to the PDA formation process and the coating-substrate interaction, as discussed below. DFT calculations[23,24] and experimental[25] studies have shown that dopamine molecules coordinate nearly perpendicularly to TiO_2 substrates, with the catechol moiety oriented toward the surface. This potentially enables the formation of a tight packing of dopamine monomers on titanium surfaces at the early stages of the PDA layer formation process, consequently resulting in a maximized interaction at the titanium-PDA interface. In addition, the catechol-TiO_2 interaction has been proven to be quite unique. Lee and co-workers[26] showed by using single molecule mechanics that the catechol molecules form fully reversible bonds with titanium substrates. The dissociation strength between a catechol molecule and the titanium surface measured in the particular study was weaker than a covalent bond, however roughly one order of magnitude stronger compared to hydrogen bonding. Thus, the excellent affinity of catechol moieties with TiO_2 substrates, renders polydopamine-based coatings an attractive option when it comes to titanium surfaces.

In certain cases PDA by itself does not provide the desired performance at interfaces. Wherein such cases the addition of functional molecules during the polymerization of dopamine offers the opportunity to tune the chemistry and by extent the functionality of PDA-based films.[27] As an example, Lenhart and co-workers[28] co-polymerized aminopropyl triethoxy silane (APTES) and dopamine to form modified PDA (SiPDA) films. APTES and PDA were combined on the basis that APTES would bond with the adhesive, while the catechol moieties would provide adhesion with the substrate in the presence of water.[28] In a later work[29] SiPDA coatings were applied as structural adhesives in aluminium-epoxy joints that were tested in dry conditions and after exposure in a hot/wet environment. Even though the authors noted an increase in the durability of the joints when using SiPDA, they concluded that SiPDA coatings are not suitable for structural adhesive applications due to their likely poor shear properties.[29] However, the attempts to apply SiPDA coatings as structural adhesives are elucidated in one study and thus for one material system. This leaves the applicability of these coatings in different systems and processing conditions still an open question.

In our study, we address the adhesion instability after hot/wet conditioning between titanium and high-performance TPCs by forming SiPDA layers on the titanium surface before the joining process. More specifically, a C/PEKK composite tape and the coated titanium alloy were bonded via a co-consolidation process to form mandrel peel test specimens. Afterward, the titanium-C/PEKK fracture toughness was evaluated by mandrel peel testing before and after hot/wet conditioning.

2. Results

2.1. Mandrel Peel Test and Fractured Surface Analysis

The adhesion between C/PEKK and titanium was quantified using mandrel peel testing. **Figure 1**a shows an example of the effective peel force, which is the difference between the peel force (F_p) and the alignment force (F_a), as a function of the displacement (see section 5.5). The blue line corresponds to the peel experiment, in which the two adherents were de-bonded. The orange line corresponds to the subsequent friction measurement test, used to correct the effective peel force, before determining the critical energy release rate G_c. The effective peel force value initially increased until the crack started to propagate, where it reached a plateau value. The fracture toughness was calculated (see section 5.5) by averaging the G_c values

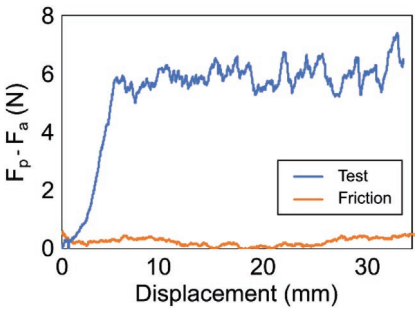

Figure 1. Representative example of effective force versus displacement curve obtained from testing a mandrel peel specimen.

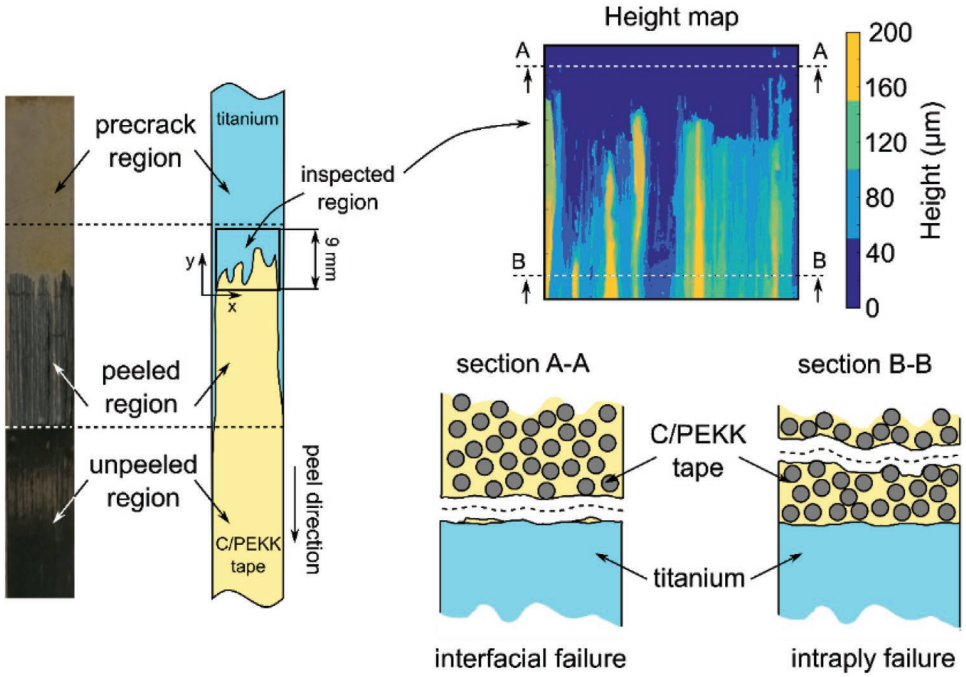

Figure 2. Top view of a mandrel peel specimen after testing and a height map of the crack surface with highlighted areas of interfacial failure (section A-A) and intra-ply failure (section B-B).

over the plateau region for displacement values between 10 and 30 mm for each specimen.

Figure 2 depicts a schematic example of a titanium surface after the peel test. Two different regions can be distinguished by visual inspection: the region where the titanium surface is visible and where part of the composite tape remains bonded onto the titanium substrate. The former indicates interfacial failure, and the latter corresponds to intra-ply (cohesive) failure. In case of intra-ply failure, the crack no longer propagated at the titanium-C/PEKK interface but deflected in the composite ply.[10] Height maps of crack surfaces were obtained via digital microscopy to visualize the extent of interfacial and intra-ply failure for each sample; an example image is shown in Figure 2. It should be noted that when intra-ply failure is predominant, the G_c value approaches the interlaminar fracture toughness of UD C/PEKK laminates, which is 1.4 kJ m^{-2}.[14] This value is the highest toughness achieved with this material system and test method. The intra-ply failure primarily involves fiber-matrix failure,[10] which is the same failure mechanism observed for the UD C/PEKK laminates subjected to mode I crack opening.[30] Thus, interfacial G_c values that approach or exceed the fracture toughness of UD C/PEKK laminates cannot be quantified but only qualitatively evaluated from the extent of intra-ply failure.

2.2. Effect of Surface Modification

2.2.1. Short Term Conditioning

Different coatings were applied on the surface of titanium before the co-consolidation process to improve adhesion and durability between PEKK and titanium. **Figure 3** summarizes the peel test results of dry and wet-conditioned as-received, APTES, PDA, and $SiPDA_{3:2}$ samples. The subscript 3:2 indicates the APTES:dopamine ratio used to for the SiPDA film formation process. Figure 3 shows that all utilized surface modifications significantly enhanced G_c values in dry conditions when compared to the as-received samples. In addition, all surface modified samples showed intra-ply failure for all surface modified samples, in contrast to the as-received sample, which exhibited interfacial failure. These findings indicate that all applied surface modification approaches provide strong interactions with the native oxide surface of the titanium strip and form bonds with PEKK during the co-consolidation process.

After hot-wet conditioning for 24 h, the unmodified samples showed a small drop of G_c, while a significant drop of G_c was observed for the APTES and PDA-modified samples. The decrease of G_c for APTES and PDA modified samples is reflected in a transition from intra-ply to interfacial failure. This observation suggests that both modification methods did not promote bond stability at the joint interface, in the presence of moisture. Remarkably, the co-deposition of APTES and PDA resulted in a G_c value comparable to the G_c of UD C/PEKK laminates in dry conditions. In addition, the G_c value and failure mechanism (intra-ply) were retained after 24 h in hot-wet conditions. Overall, the $SiPDA_{3:2}$ layer provided the best adhesion and moisture resistance out of the used surface modifications.

2.2.2. Long Term Conditioning

$SiPDA_{3:2}$ peel samples were kept in the conditioning chamber for exposure times up to 1440 h (≈2 months) to evaluate the

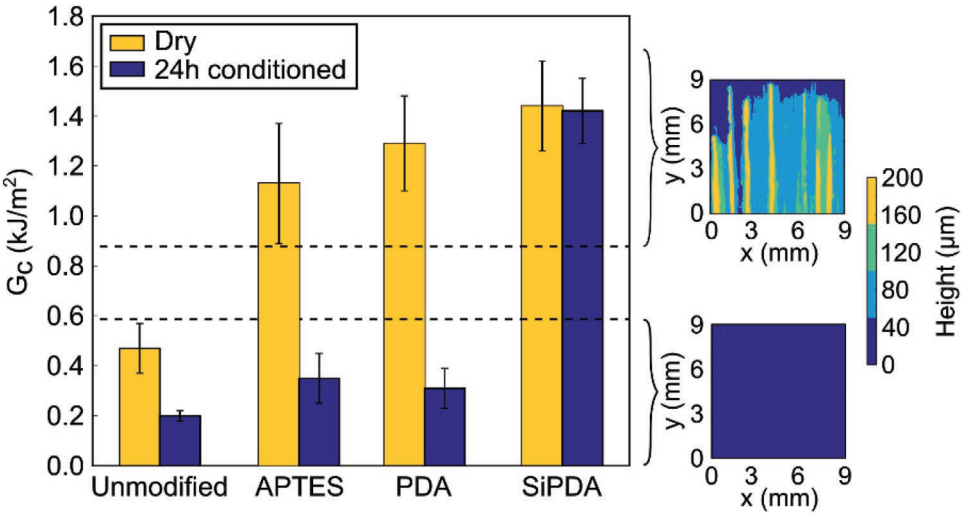

Figure 3. Fracture toughness values and failure modes of the samples tested after dry conditioning and after 24 h of exposure to hot/wet (70 °C, 80% RH) environment. The toughness values reported for the unmodified sample are reproduced from ref. [18].

long-term performance of the coatings. The results of the long-term exposure study are shown in **Figure 4**A in terms of fracture toughness as a function of conditioning time. It is evident that after 24 h the toughness slightly decreased from 1.4 kJ m^{-2} to roughly 1.2 kJ m^{-2} and then similar values were maintained until a conditioning time of 480 h. Subsequently, a more pronounced bond degradation occurred, as the measured toughness dropped to a value of 0.42 kJ m^{-2} for a conditioning time of 1440 h. The results of the fractured surface analysis, depicted in Figure 4B, reflect the fracture toughness values. A predominant intra-ply failure is observed until a conditioning time of 240 h. For the samples conditioned for longer time, the amount of intra-ply failure decreased, until the sample exhibited predominantly interfacial failure (see Figure 3) after a conditioning time of 1440 h.

2.2.3. The Effect of APTES:Dopamine Ratio

The influence of different APTES:dopamine (A:D) ratios on the moisture resistance of the titanium-C/PEKK joints was also evaluated. **Figure 5**A shows the mandrel peel test results of the samples prepared using different A:D ratios. In dry conditions, all compositions investigated here exhibited similar G_c values of ≈1.4 kJ m^{-2}. As previously pointed out, these toughness values are comparable to the fracture toughness of C/PEKK laminates. Thus, it is impossible to distinguish whether the different compositions result in different adhesion values in dry conditions as the interface is not the weakest link under the loading condition used in this study. After hot/wet conditioning, it is evident that increasing the amount of APTES promotes adhesion stability. The $SiPDA_{1:2}$ sample shows weak adhesion and,

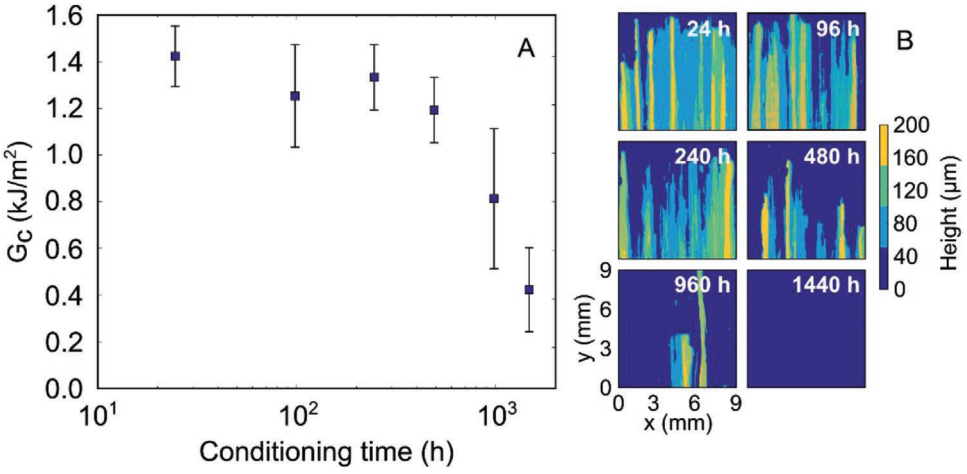

Figure 4. Results of the long-term exposure study in terms of fracture toughness versus conditioning time in hot/wet (70 °C, 80% RH) environment, conducted on $SiPDA_{3:2}$ modified samples (A). Height map of the crack surfaces of $SiPDA_{3:2}$ modified sample after 24, 96, 240, 480, 960, and 1440 h conditioning in hot/wet (70 °C, 80% RH) environment (B).

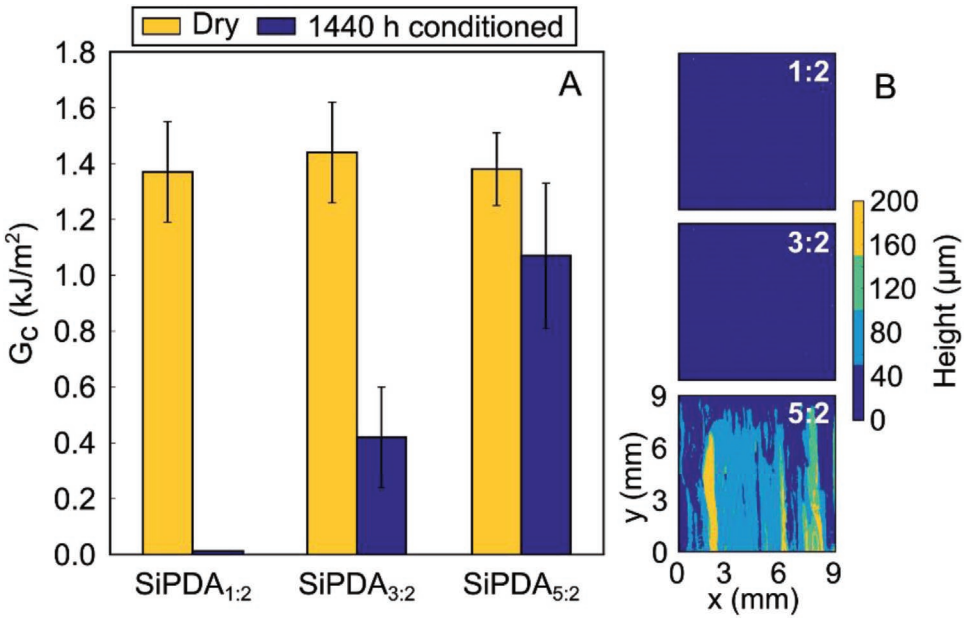

Figure 5. Fracture toughness values the samples modified using different APTES:dopamine ratios. The samples were tested after dry conditioning and after 1440 h of exposure to hot/wet (70 °C, 80% RH) environment (A). Example of height map of the crack surface of SiPDA$_{1:2}$, SiPDA$_{3:2}$ and SiPDA$_{5:2}$ modified specimens exposed to hot/wet (70 °C, 80% RH) environment for 1440 h.

generally, premature failure of the specimens prior to testing, while the SiPDA$_{3:2}$ coating enabled to retain 30% of the toughness measured in dry conditions. Finally, the SiPDA$_{5:2}$ coating provided the best performance, as 75% of the toughness was retained, and a predominant intra-ply failure was observed.

Overall, from the fracture surface analysis (Figure 5B) of the SiPDA samples, it is evident that SiPDA$_{1:2}$ and SiPDA$_{3:2}$ exhibit an interfacial failure after hot/wet conditioning, while the SiPDA$_{5:2}$ shows a partial intra-ply failure. However, it is impossible to identify the location of the interfacial failure with respect to the SiPDA nano-layers by using optical microscopy. This is due to the fact that the thickness values of the SiPDA coatings are below the detection limit of the optical microscope. Therefore, the fracture surfaces were analyzed via X-ray photoelectron spectroscopy (XPS). More particularly, XPS measurements were performed on both titanium and C/PEKK surfaces in the regions that exhibited interfacial failure. The maximum information depth of XPS when using an aluminium source is 9–10 nm,[31] while the applied coatings have an estimated thickness of ≈90 – 100 nm (see Supporting Information S1). This implies that if the interfacial failure occurs at/or close to the titanium-SiPDA interface, then (at the titanium fractured surface) it is possible to measure a titanium atomic concentration similar to the as-received titanium surface. However, if interfacial failure occurs at the PEKK-SiPDA interface, no titanium should be traced since the remaining layer's thickness exceeds the information depth of XPS.

Figure 6 shows the XPS spectra from the fractured surfaces of SiPDA$_{1:2}$, SiPDA$_{3:2}$, and SiPDA$_{5:2}$ samples. The upper graphs (B_1–B_3) show the spectra obtained from C/PEKK, while the lower graphs exhibit (C_1–C_3) the spectra obtained from titanium. The titanium peak is clearly observed in the XPS spectrum from the titanium side of the SiPDA$_{1:2}$ and SiPDA$_{3:2}$ samples. The atomic surface concentration of Ti is 13.4% and 11.7% for SiPDA$_{1:2}$ and SiPDA$_{3:2,}$ respectively, slightly lower than the one of the as received titanium surface, that is, 14.7% (see Supporting Information S4.1). In addition, in the XPS spectra from the PEKK side for the SiPDA$_{1:2}$ and SiPDA$_{3:2}$ samples, Si can be traced which is not present in the C/PEKK tape (see Supporting Information S4.1). Based on this, we conclude that for the SiPDA$_{1:2}$ and SiPDA$_{3:2}$ samples, after conditioning the bonded interfaces for 60 days and then fracturing them, interfacial failure occurs at the titanium-SiPDA coating, with only traces from the coatings remaining on the surface.

Conversely, in the XPS spectrum from the titanium side of the SiPDA$_{5:2}$ sample, the signal of the Ti peak is significantly lower compared to the SiPDA$_{1:2}$ and SiPDA$_{3:2}$ samples, with a Ti atomic concentration of 1.5%. The main elements traced on the titanium surface of SiPDA$_{5:2}$ are C, O, and Si, as well as small amounts of N. In the spectrum from the PEKK side the SiPDA$_{5:2}$ sample, C, O, N, and Si elements can be traced. However, the atomic concentration of Si is lower when compared to the titanium side, that is, 4.9% and 2.2% for the titanium and PEKK surface, respectively. Based on the above observations, we hypothesize that the interfacial failure occurs predominantly at the PEKK-SiPDA interface. However, because the SiPDA$_{5:2}$ sample exhibits high fracture toughness values, the failure seems to be unstable resulting sporadically in a cohesive failure of the SiPDA$_{5:2}$ coating making the detection of traces of Ti possible. For a visual representation please see the inserts in Figure 6B_3,C_3.

3. Discussion

3.1. SIPDA Coatings for Tough and Hot/Wet Conditioning Resistant Pekk/Ti Interfaces

APTES, PDA, and SiPDA coatings were demonstrated to promote adhesion in co-consolidated C/PEKK-titanium joints

ADVANCED MATERIALS INTERFACES
Open Access
www.advmatinterfaces.de

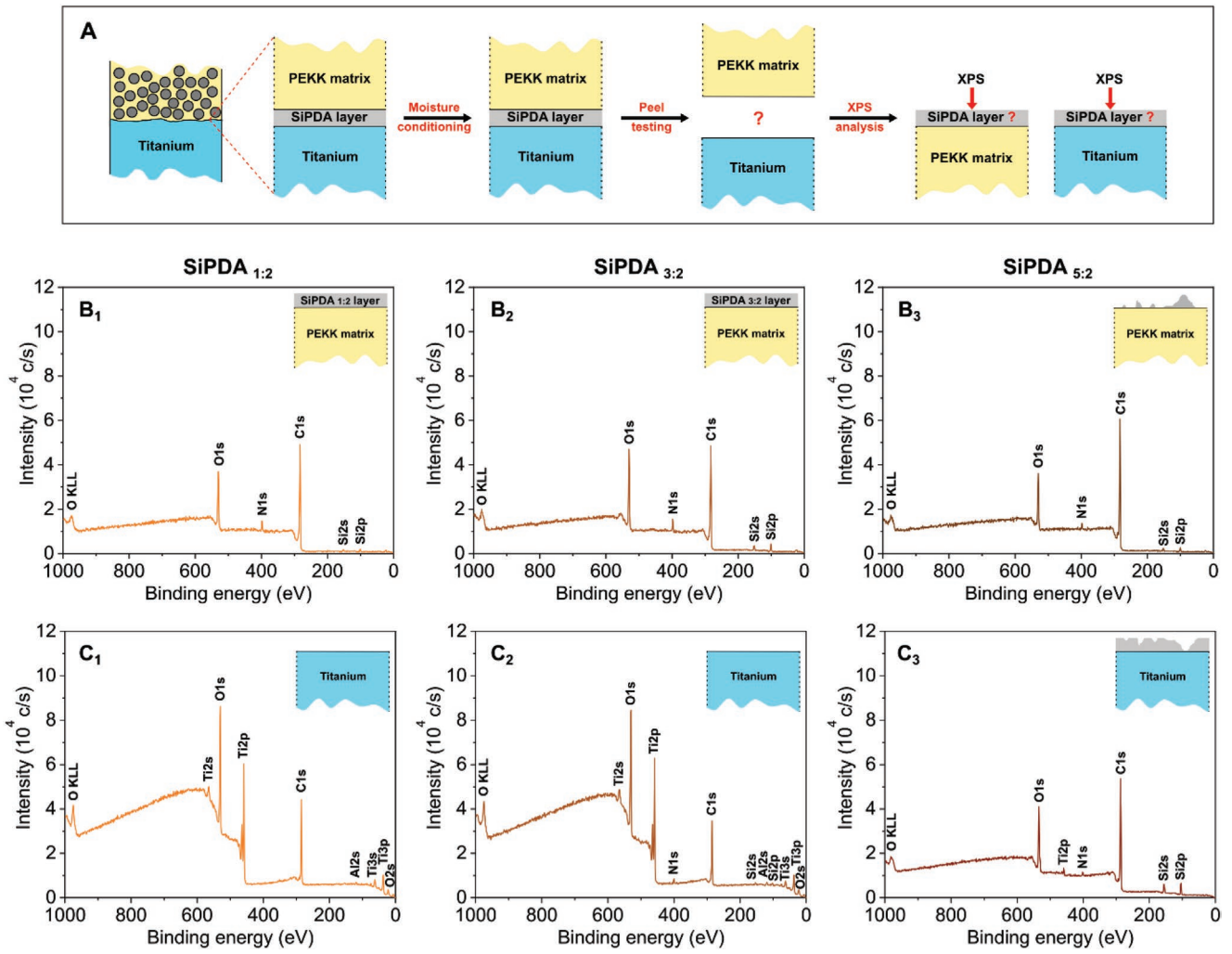

Figure 6. Schematic representation of the sample preparation for XPS analysis (A). XPS spectra were obtained from the fractured surfaces of C/PEKK (B1–B3) and titanium (C1–C3). The spectra originate from $SiPDA_{1:2}$, $SiPDA_{3:2}$, and $SiPDA_{5:2}$ samples that were tested via mandrel peel after 1440 h conditioning. The atomic concentration values for each spectrum can be found in supporting information (Supporting Information S4.1).

in dry conditions. However, despite the great performance of the coated samples in dry conditions, a significant interfacial toughness drop was observed for certain surface modifications after 24 h of conditioning (see Figure 3). It is worth mentioning that the geometry of a mandrel peel test coupon allows easy water access to the interface. In particular, a composite tape of the same thickness as the one used in our study, can be saturated within 24 h[18] under the same conditioning parameters. This means that water will reach the titanium-coating-PEKK interphase after 24 h conditioning. Thus, the question is what determines the performance of each of the applied coatings concerning adhesion after hot/wet conditioning.

APTES is estimated to form a layer of roughly 1 nm (see Supporting Information S1) and the Si—O—Ti bond that forms with titanium substrates has been shown to be prone to hydrolysis.[32] Based on these reported results we hypothesize that the APTES layer does not perform well after hot-wet conditioning for two reasons. The APTES layer is hydrolytically unstable, and due to its small thickness, it does not prevent water from reaching the interface.

Considering the PDA layer, it is estimated to have a thickness of ≈80 nm (see Supporting Information S1), which is 1–2 orders of magnitude higher than the thickness than that of APTES. Using XPS measurements and the methodology described in section 2.2.3, it is shown that after 24 h conditioning, interfacial failure occurs at and/or close to the titanium-PDA interface (please refer to Supporting Information S4.2 for further details), which is evidently the weakest link. Hence, we hypothesize that water molecules diffuse through the PDA layer and the composite ply to weaken the bonds between the catechol moieties and the native titanium oxide. This reasoning is supported by DFT molecular dynamic simulations, estimating a decreased adsorption energy of catechol moieties in the presence of water,[33] as well as the previously reported competition between water molecules and oxygen-containing organic species in binding at TiO_2 surfaces.[34] Hence, the presence of water molecules at the PDA-titanium interface would result in a significantly weakened interaction, which could explain the poor adhesive performance observed after 24 h hot/wet conditioning.

As shown in section 2.2.3 the $SiPDA_{3:2}$ layer, exhibits a similar behavior with PDA after moisture conditioning, that is, it

fails at and/or close to the SiPDA-titanium interface. However, the transition from an intra-ply to a 100% interfacial failure occurs at different timescales for PDA and $SiPDA_{3:2}$ samples, that is, ≈24 and ≈1440 h, respectively. Thus in both cases hot/wet conditioning mainly impacts the titanium-coating interface, which eventually determines the overall durability of the titanium-C/PEKK joint. Since both PDA and SiPDA samples show the same failure mechanism after hot/wet conditioning, it is reasonable to assume that water diffusion through the nanolayers determines the timescale to transition from an intra-ply to an interfacial failure. Hence we propose that the addition of APTES during the polydopamine formation process, in combination with the processing conditions used to produce the joints (T = 375 °C, P = 6 Bar), results in a layer that exhibits a significantly reduced water permeability.

By changing the A:D ratio for conditioning times of 1440 h, a clear increasing trend of G_c with the A:D ratio is observed. Thus by incorporating more silane into the PDA structure, resistance to hot/wet conditioning increased. The important aspect to highlight is the notable change observed in the failure mode with respect to the SiPDA layer. In contrast to $SiPDA_{1:2}$ that exhibits an identical failure mechanism with $SiPDA_{3:2}$ and PDA, $SiPDA_{5:2}$ fails in a different fashion. The failure mode of $SiPDA_{5:2}$ sample indicates that the $SiPDA_{5:2}$-titanium interface is not the weakest link after hot/wet conditioning for 1440 h. In this case failure seems to occur close to the PEKK-$SiPDA_{5:2}$ interface in an unstable fashion, while the measured G_c values of the joint remain above 1 kJ m^{-2}. The latter can be also an indication of the weak impact of hot/wet conditioning on the bonding at the $SiPDA_{5:2}$-PEKK interface, as well as the cohesive strength of the $SiPDA_{5:2}$ layer, at least within the considered timescale.

The notion that SiPDA coatings have the potential to provide enhanced performance in polymer-metal joints after conditioning has been previously introduced by Lenhart and co-workers.[28] In the particular study, SiPDA coatings were first synthesized aiming to have catechol moieties to improve adhesion with the substrate in the presence of water molecules, while APTES would promote bonding with the adherent. In the present work, the results suggest a different functionality of the SiPDA layers. Based on the observed G_c values shown in section 2.2, strong adhesion is assumed for APTES, PDA and SiPDA coatings with both the adherent and the adhesive, that is, titanium and PEKK, respectively. In addition, PDA and APTES did not show a significant hot/wet conditioning resistance in contrast to SiPDA. Thus, we proposed that the hot/wet conditioning resistance provided by SiPDA coatings is related to their water permeability. However, PDA-based coatings are expected to thermally transform at the processing temperature (375 °C) used in this study. TGA and FTIR measurements provide an indication of the thermal transformation of PDA and SiPDA (see Supporting Informations S2 and S3). Thus the initial hypothesis of Lenhart and co-workers[28] potentially holds when Si-PDA layers are applied in a different materials system and/or processing conditions.

3.2. Polydopamine-Based Coatings as Structural Adhesives

Despite the successful application of PDA-based coatings in a broad range of fields,[35–38] the suitability of PDA and SiPDA layers as structural adhesives has been recently questioned.[22,29] The main argument to explain why such coatings do not perform well in that context, is associated with their poor mechanical properties.[22,29] However, in this work we show that when titanium is bonded to PEKK via a co-consolidation process, the deposition of PDA and SiPDA layers on the titanium surface before the joining process resulted in an interphase that was not the weakest link. This holds for both types of coatings when testing after storage in dry conditions. Thus it is of importance to understand why the PDA-based layers considered in this work performed remarkably well as adhesive interlayers.

The high G_c values promoted by PDA and SiPDA coatings in samples stored in dry conditions, indicate strong bonding of the coatings with both titanium and PEKK. In the case of titanium, this could be accounted to the well-known strong interaction between the titanium oxide and catechol moieties present in PDA-based coatings.[26,39] It should be also noted that the strong bonding of the PDA and SiPDA coatings with titanium is demonstrated after being subjected to processing temperatures of 375 °C. This highlights the relevance of the thermal stability of PDA-based coatings in adhesion applications. In the case of PEKK, identifying the interaction with the applied coatings remains a challenge. It is plausible that the heat and pressure of the co-consolidation process resulted in the formation of bonds between the PDA-based layers and PEKK. Some possibilities may include aryl coupling and Michael-type addition, reactions that have been identified as bond formation mechanisms in catechol-based chemistry.[40,41]

When it comes to what is considered the Achilles heel of PDA-based coatings, that is, the poor mechanical properties,[22,29,42] joining processes that use high temperatures can offer a distinct advantage. This is due to the thermal transformation that PDA experiences upon heating, as reported by numerous studies.[43–51] Thermal annealing of PDA, has been shown to have a positive impact on the mechanical properties of the coatings by scratch[52] and nano-indentation[53] tests. The same holds for SiPDA coatings, as nano indentation tests indicate a significant decrease of the maximum indentation depth after annealing at 375 °C (see Supporting Information S5). Such an effect can be beneficial for high-performance thermoplastics that require high processing temperatures, resulting in joining the thermoplastic polymer with metals and improving the mechanical properties of PDA-based coatings used to promote adhesion.

Due to the specifics of each individual polymer-metal joint where PDA-based coatings were applied, it is not feasible to conclude why they have failed to qualify as a structural adhesives. Nonetheless, we report the first successful application where PDA and SiPDA layers exhibited a remarkable performance under the loading conditions introduced by mandrel peel testing. PDA coatings were shown not only to greatly promote adhesion processing conditions including high temperatures and pressures, but also provide functionality by the incorporation of molecules in the PDA structure. This highlights the potential of PDA layers to provide a base for tailoring interfacial properties and could offer an application window to be considered as adhesives in high-performance hybrid materials.

4. Conclusions

In this work we have demonstrated the potential of polydopamine (PDA)-based coatings to promote tough and hot/wet conditioning resistant interfaces in titanium-PEKK co-consolidated joints. PDA and SiPDA layers were deposited on the surface of titanium before the co-consolidation process with PEKK. The interfacial fracture toughness (G_c) of the co-consolidated joints was evaluated via mandrel peel tests after storing the samples in dry or hot/wet conditions. In dry conditions, both PDA and SiPDA coatings resulted in a greatly increased G_c value, close to the fracture toughness of the PEKK composite tape, that is, 1.4 kJ m^{-2}. The PDA treated samples exhibited a sharp decrease of G_c after 24 h of exposure in hot/wet conditions that was attributed to the weakening of the titanium-PDA interface in the presence of water molecules. Conversely, SiPDA layers provided an exceptional resistance to hot/wet conditioning that depended on the silane content. Based on the observed interfacial failure mechanism, it was hypothesized to be the result of a decreasing water diffusivity through the SiPDA layers by increasing the silane content. In terms of resistance to hot/wet conditioning, the best performing coating was $SiPDA_{5:2}$ that exhibited G_c values above 1 kJ m^{-2} even after 60 days storage in hot/wet environment. Overall, PDA-based layers were shown to promote adhesion and introduce functionality at interfaces, even at high temperatures and pressures during processing. This highlights the potential of PDA chemistry to be applied in high-performance composite materials and structures.

5. Experimental Section

Materials: Dopamine hydrochloride (M: 189.64 g mol^{-1}), tris(hydroxymethyl)-aminomethane buffer (M: 121.14 g mol^{-1}) and (3-aminopropyl)triethoxysilane (APTES, M: 221.37 g mol^{-1}), were purchased from Sigma-Aldrich (Zwijndrecht, the Netherlands). Toluene, acetone, and 2-propanol were purchased from VWR (Amsterdam, the Netherlands). Marbocote 227-CEE releasing agent was purchased from Fatol (Hengelo, the Netherlands). Titanium grade 5 (Ti6Al4V) was supplied by Singeling B.V. in laser cut strips (120 × 10 × 2 mm^3) suitable to the mandrel peel test sample geometry and having a surface roughness of 0.6 µm. Toray Advanced Composites kindly provided PEKK (Kepstan 7002) film with a thickness of 50 µm. Carbon fiber-PEKK (C/PEKK) pre-impregnated tape (Cetex TC1320) was supplied by Toray Advanced Composites. The C/PEKK tape consisted of unidirectional carbon fibers (AS4) and PEKK matrix, it had a fiber volume fraction of 59% and a thickness of 0.15 mm.

Surface Modification of Titanium Strips: The titanium strips were ultrasonically solvent-cleaned (2510 ultrasonic cleaner; Branson, Danbury, USA) in the following sequence of solvents: toluene, acetone, 2-propanol, and water (Milli-Q Advantage A10, Millipore), for 30 min per solvent. After cleaning, the strips were dried under vacuum at 50 °C for 24 h (VOS-12051, VOS instruments, the Netherlands). The strips subjected to the cleaning process will be referred to as "as-received."

In a typical polydopamine (PDA) coating process, 14 titanium strips were treated with oxygen plasma (Plasma Prep II SPI; West Chester, USA) for 1 min using a current of 40 mA and an oxygen pressure of 200 mTorr. Immediately after plasma treatment the strips were placed perimetrically, in a vertical position, in a 400 mL beaker containing a freshly prepared tris-buffer (10 mM, pH = 8.5) – polydopamine (5 mg mL^{-1}) solution and left there for 24 h under vigorous stirring. After the coating process, the strips were thoroughly cleaned with Milli-Q water to remove any traces of weakly bound PDA aggregates on the formed PDA film and were then dried under vacuum at 40 °C (VOS-12051, VOS instruments, the Netherlands) for 24 h. The PDA-modified strips were stored under vacuum at room temperature until they were used for the co-consolidation process (see section 5.4). It should be noted that the surface of the modified strips used to bond with the C-PEKK tape was the one facing inward during the PDA deposition process.

APTES was deposited at the surface of titanium strips using an aqueous APTES solution of 1% v/v. Before deposition, the titanium strips were cleaned, treated with plasma, and positioned in the APTES solution similarly to the PDA samples.

For the APTES-PDA (SiPDA) coatings, three different APTES:Dopamine (A:D) molar ratios were employed, that is, 1:2, 3:2, and 5:2. The term SiPDA denoted silicon containing PDA layers. The coating process for SiPDA was similar with the one mentioned for PDA, with three distinct variations. The variations were the dopamine concentration (2.5 mg mL^{-1} instead of 5 mg mL^{-1}), the addition of APTES and the immersion times of the titanium strips in the APTES-dopamine solution for the different molar ratios, that is, 24 h for the A:D ratio of 1:2 ($SiPDA_{1:2}$), 8 h for the A:D ratio of 3:2 ($SiPDA_{3:2}$), and 4 h for A:D ratio of 5:2 ($SiPDA_{5:2}$).

PDA and SiPDA Characterization: For characterization purposes, PDA and SiPDA coatings were deposited on a silicon (SiO_2) wafer and a silicon wafer coated with a ≈50 nm titanium oxide (TiO_2@SiO_2) layer.

The PDA and SiPDA coated TiO_2@SiO_2 wafers were cut using a diamond pen. Then the cross-section of the wafers at the location where the layer was formed was imaged using scanning electron microscope (JSM 7610 FPlus; JEOL) to estimate the thickness of the formed layers. The acceleration voltage was 1.5 kV and the measurements were performed at a working distance (W.D.) of 7.9 mm. The average thickness of the formed PDA and SiPDA layers was determined by the average of at least 5 samples.

The PDA and SiPDA coated SiO_2 wafers were analyzed via infrared spectroscopy (Alpha, Bruker) in transmission mode to gain insights on the chemical structure of the layers formed. The spectrum was obtained from 4000 to 400 cm^{-1} with a resolution of 4 cm^{-1} and the result was an average of 64 scans. The final spectrum was then smoothened (25-points) and subjected to a baseline correction.

Thermogravimetric analysis (TGA, TGA550, TA instruments) was performed on PDA and SiPDA powders to identify their thermal stability. To obtain the PDA and SiPDA powders, the post polymerization solution of each respective composition was centrifuged (Z36HK, HERMLE Labotechnik, Germany) to isolate the precipitates formed, which were then redispersed in Milli-Q water. The process was repeated five times and the powders were dried for 24 h under vacuum at 40 °C (VOS-12051, VOS instruments, the Netherlands). TGA was then performed on PDA, $SiPDA_{1:2}$, $SiPDA_{3:2}$, and $SiPDA_{5:2}$ powders from 25 to 600 °C at a rate of 10 °C min^{-1} in N_2 atmosphere.

To evaluate the thermal transformation of PDA and SiPDA layers, FTIR measurements were performed on dry PDA and SiPDA powders, as well as on powders annealed at 375 °C. The annealed powders were obtained by placing them in the TGA apparatus and heating them from 25 to 375 °C at a rate of 10 °C min^{-1}, followed by an isothermal at 375 °C for 180 min. FTIR spectra were obtained from 4000 to 400 cm^{-1} with a resolution of 4 cm^{-1} and the results represent averages of 64 scans. The final spectra were then smoothened (25-points) and subjected to a baseline correction.

Nanoindentation (Anton Paar NHT^2 nano indenter, ST Instruments, Groot-Ammers, the Netherlands) tests were performed on as produced and thermally treated $SiPDA_{3:2}$ coated SiO_2 wafers to provide insights on the effect of thermal treatment on the mechanical properties of the coatings. To ensure that the indentation depth does not exceed the thickness of the coatings multiple deposition steps (according to section 5.2) were performed on SiO_2 wafers. The coated wafers were then cut using a diamond pen into 8 × 8 mm squares and were either used as deposited or were thermally treated in N_2 atmosphere using the TGA apparatus from 25 to 375 °C at a rate of 10 °C min^{-1}, followed by an isothermal scan at 375 °C for 180 min. The final thickness of the coatings

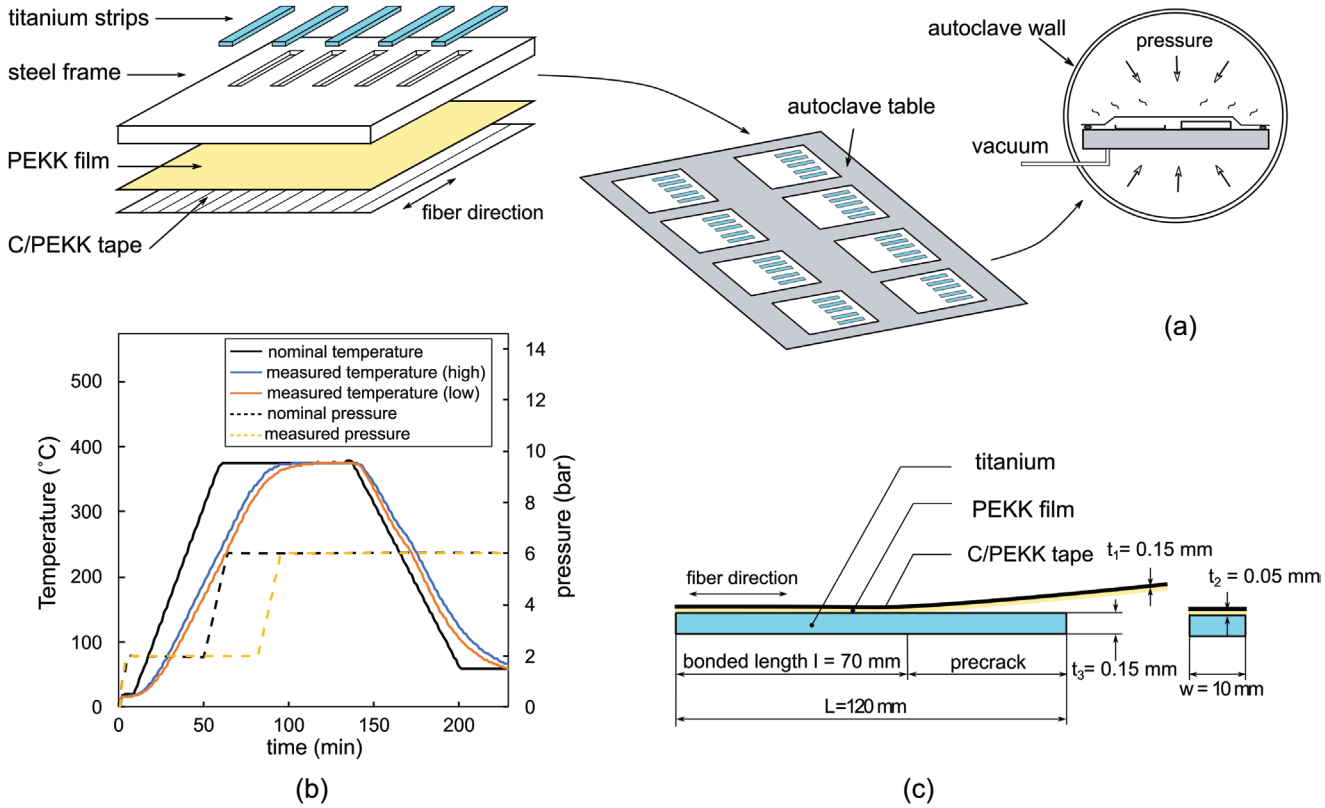

Figure 7. a) Schematic representation of the mandrel peel sample preparation, b) Autoclave cycle used to co-consolidate the mandrel peel samples. The solid lines represent the temperature profile (nominal and measured). The dashed lines represent the pressure profile (nominal and measured), c) Dimensions and geometry of a titanium-C/PEKK mandrel peel sample.

subjected to testing was evaluated by the means of cross-sectional SEM imaging (see first paragraph of this section). The nano-indentation tests were performed using a conical tip and more than 10 measurements were performed per sample category. The testing mode was in load control at a maximum load of 500 µm with the loading, holding, and unloading segments to be 30 sec.

The film thickness, nano-indentation, and IR spectrum of the PDA and SiPDA coatings, as well as the IR spectrum and TGA of the PDA and SiPDA powders are shown in supporting information (Supporting Informations S1–S3 and S5).

Titanium-C/PEKK Co-Consolidation and Moisture Conditioning: The peel samples, consisting of a single ply of C/PEKK tape bonded to the surface modified titanium strips, were prepared using a vacuum bag which was subjected to an autoclave co-consolidation process.[14] First, the C/PEKK tape and the PEKK film were dried at 100 °C for 24 h to remove any moisture.[54] Afterward, the C/PEKK followed by the PEKK film and the titanium strips (modified according to section 5.2) were placed on a flat table. The PEKK film was added between the two adherends (C/PEKK & titanium) to ensure sufficient wetting of titanium by the PEKK matrix. A steel frame was used to ensure a good alignment between the length of the strips and the fiber direction, as schematically represented in **Figure 7**a. The releasing agent was applied to the steel frame to avoid adhesion of PEKK to the alignment frame. The same release agent was also applied to the first 50 mm of the titanium strips to obtain an initial pre-crack, which is required by the mandrel peel test. The table was wrapped in a vacuum bag to conduct the co-consolidation in an autoclave at 6 bar pressure and a dwell temperature of 375 °C. The temperature and pressure profile over the entire cycle are shown in Figure 7b. A schematic representation of the obtained samples is depicted in Figure 7c. The resulting peel samples prepared using as received, PDA-, APTES-, $SiPDA_{1:2}$-, $SiPDA_{3:2}$-, and $SiPDA_{5:2}$-coated titanium strips, from now on will be referred as "unmodified," "PDA," "$SiPDA_{1:2}$," "$SiPDA_{3:2}$," and "$SiPDA_{5:2}$."

Two different groups of samples were considered in this work. The first one was noted as dry sample, as the specimens were tested soon after the de-molding, giving no time for water diffusion. The second one was noted as wet-conditioned sample, as the specimens were stored in a conditioning chamber before mechanical testing. The conditioning chamber was kept at 70 °C and 80% of relative humidity. Considering that the geometry of the mandrel peel sample allows a quick diffusion of water to the interface,[16] the effect of moisture on the adhesion was conducted by conditioning the samples for times ranging from 24 to 1440 h.

Mechanical Characterization: A mandrel peel test was used to assess the interfacial fracture toughness G_c as a measure of the degree of adhesion. It was demonstrated to be suitable to assess the adhesion in metal-composite systems measured as the plastic work that occurs in the composite arm during peeling.[55] Similar to a 90° peel test, the presence of a mandrel ensured the composite peel arm to have a constant large radius of curvature, thereby preventing its breakage during testing.

Figure 8 schematically represents the configuration of the mandrel peel test setup, which was installed in a Zwick universal testing machine. The titanium side of the specimen was fixed on a sliding table, and the composite arm was bent around a cylindrical mandrel with a diameter of 10 mm. A tensile force F_p was applied to the composite arm to peel it from the titanium using a constant displacement rate of 15 mm min^{-1}. A constant alignment force F_a of 60 N, applied to the sliding table via a pneumatic actuator, ensured that the peel arm conformed to the mandrel. Both peel and alignment force were recorded using two 200 N load cells. The energy release rate G was calculated as:[30]

$$G = \frac{1}{w}\left[F_p(1-\mu) - F_a\right] \quad (1)$$

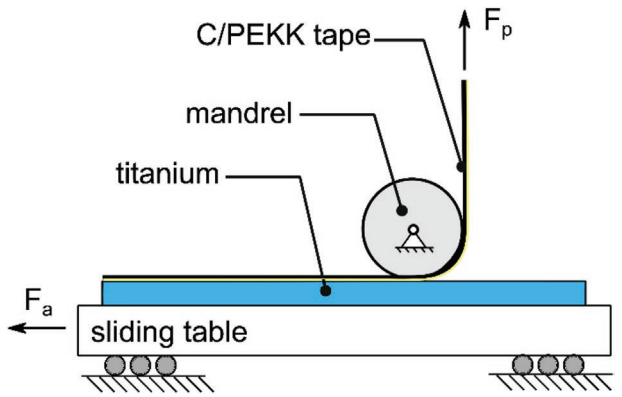

Figure 8. Illustration of the mandrel peel test setup.

in which w is the width of the specimen and μ is the friction coefficient of the setup. A second peel experiment was performed on a de-bonded specimen to evaluate the coefficient μ. By measuring F_p and F_a, from Equation (1) and $G = 0$ a coefficient μ of 0.007 was found. The final G_c value is averaged out of five specimens per sample category.

Identification of Failure Location: The mandrel peel test was followed by a crack surface analysis conducted at two different length scales, that is, micro- and nanoscale, to determine the failure mechanisms.

The micro-scale analysis was carried out using a digital microscope (Keyence VHX-7000) to identify whether the respective sample groups failed at the titanium-composite interface (interfacial failure) or within the composite ply (intra-ply failure). The nano-scale analysis was performed for the samples that showed interfacial failure using X-ray photoelectron spectroscopy (XPS, PHI Quantes, Physical Electronics) to identify where the failure occurred with respect to the PDA-based coatings. More specifically, the samples examined were the as-received and PDA after conditioning (see section 5.4) for 24 h as well as the $SiPDA_{1:2}$, $SiPDA_{3:2}$, and $SiPDA_{5:2}$ after conditioning (see section 5.4) for 1440 h. For each sample group, XPS was performed on both the titanium and C/PEKK using a monochromatic Al Ka source at 1486.6 eV with a beam diameter of 100 µm, an X-ray gun power of 25 W and the beam and detector input angles were 45°. The base chamber pressure was 7×10^{-7} Pa and the working pressure was 1.3×10^{-6} Pa (Argon). At least three different locations were measured per sample group. To provide a frame of reference, using the same parameters, XPS was also performed on the as received, PDA and SiPDA coated titanium strips before the co-consolidation process.

Supporting Information

Supporting Information is available from the Wiley Online Library or from the author.

Acknowledgements

G.K. and V.M.M. contributed equally to this work. This work was performed as part of the HTSM2017 research program under project number 16213, which is (partly) financed by the Dutch Research Council (NWO). The authors also gratefully acknowledge the financial and technical support from the industrial and academic partners of the ThermoPlastic Composites Research Centre (TPRC), as well as the support funding from the Province of Overijssel for improving the regional knowledge position within the Technology Base Twente initiative.

Conflict of Interest

The authors declare no conflict of interest.

Data Availability Statement

The data that support the findings of this study are available in the Supporting Information of this article.

Keywords

adhesive bonding, APTES, C/PEKK, hot/wet conditioning resistance, polydopamine, polymer-metal joint, titanium

Received: December 13, 2022
Revised: April 9, 2023
Published online:

[1] D. Gu, X. Shi, R. Poprawe, D. L. Bourell, R. Setchi, J. Zhu, *Science (80-.)*. **2021**, *372*, eabg1487.
[2] E. E. Feistauer, J. F. dos Santos, S. T. Amancio-Filho, *Polym. Eng. Sci.* **2019**, *59*, 661.
[3] J. Bieniaś, P. Jakubczak, B. Surowska, in *Hybrid Polymer Composite Materials*, Elsevier, Amsterdam, Netherlands **2017**.
[4] B. Kolesnikov, L. Herbeck, A. Fink, *Compos. Struct.* **2008**, *83*, 368.
[5] M. E. Kazemi, L. Shanmugam, L. Yang, J. Yang, *Composites, Part A* **2020**, *128*, 105679.
[6] S.-S. Yao, F.-L. Jin, K. Y. Rhee, D. Hui, S.-J. Park, *Composites Part B* **2018**, *142*, 241.
[7] T. K. Slange, W. J. B. Grouve, L. L. Warnet, S. Wijskamp, R. Akkerman, *Composites, Part A* **2019**, *119*, 165.
[8] D. Brassard, M. Dubé, J. R. Tavares, *Composites Part B* **2019**, *165*, 779.
[9] F. Sacchetti, W. J. B. Grouve, L. L. Warnet, I. F. Villegas, *Composites Part A* **2018**, *109*, 197.
[10] A. Pramanik, A. K. Basak, Y. Dong, P. K. Sarker, M. S. Uddin, G. Littlefair, A. R. Dixit, S. Chattopadhyaya, *Composites Part A* **2017**, *101*, 1.
[11] S. Beland, *High Performance Thermoplastic Resins and Their Composites*, William Andrew, Norwich, NY **1990**.
[12] K. Shimizu, K. Malmos, S.-A. Spiegelhauer, J. Hinke, A. H. Holm, S. U. Pedersen, K. Daasbjerg, M. Hinge, *Int. J. Adhes. Adhes.* **2014**, *51*, 1.
[13] P. Cortes, W. J. Cantwell, *J. Reinf. Plast. Compos.* **2004**, *39*, 1081.
[14] V. M. Marinosci, W. J. B. Grouve, M. B. de Rooij, S. Wijskamp, R. Akkerman, *Int. J. Adhes. Adhes.* **2021**, *109*, 102893.
[15] G. Kafkopoulos, C. J. Padberg, J. Duvigneau, G. J. Vancso, *ACS Appl. Mater. Interfaces* **2021**, *13*, 19244.
[16] A. Baldan, *J. Mater. Sci.* **2004**, *39*, 4729.
[17] K. Schulze, J. Hausmann, B. Wielage, *Procedia Mater. Sci.* **2013**, *2*, 92.
[18] V. M. Marinosci, L. Chu, W. J. B. Grouve, S. Wijskamp, R. Akkerman, M. B. de Rooij, *Composites, Part A* **2022**, *162*, 107107.
[19] C. Ingram, K. Ramani, *Int. J. Adhes. Adhes.* **1997**, *17*, 39.
[20] K. Ramani, W. J. Weidner, G. Kumar, *Int. J. Adhes. Adhes.* **1998**, *18*, 401.
[21] H. Lee, S. M. Dellatore, W. M. Miller, P. B. Messersmith, *Science (80-.)*. **2007**, *318*, 426.
[22] J. H. Ryu, P. B. Messersmith, H. Lee, *ACS Appl. Mater. Interfaces* **2018**, *10*, 7523.

[23] S. Bahri, C. M. Jonsson, C. L. Jonsson, D. Azzolini, D. A. Sverjensky, R. M. Hazen, *Environ. Sci. Technol.* **2011**, *45*, 3959.
[24] M. J. Jackman, K. L. Syres, D. J. H. Cant, S. J. O. Hardman, A. G. Thomas, *Langmuir* **2014**, *30*, 8761.
[25] S. C. Li, J. G. Wang, P. Jacobson, X. Q. Gong, A. Selloni, U. Diebold, *J. Am. Chem. Soc.* **2009**, *131*, 980.
[26] H. Lee, N. F. Scherer, P. B. Messersmith, *Proc. Natl. Acad. Sci. USA* **2006**, *103*, 12999.
[27] W. Z. Qiu, H. C. Yang, Z. K. Xu, *Adv. Colloid Interface Sci.* **2018**, *256*, 111.
[28] D. B. Knorr, N. T. Tran, K. J. Gaskell, J. A. Orlicki, J. C. Woicik, C. Jaye, D. A. Fischer, J. L. Lenhart, *Langmuir* **2016**, *32*, 4370.
[29] N. T. Tran, D. P. Flanagan, J. A. Orlicki, J. L. Lenhart, K. L. Proctor, D. B. Knorr, *Langmuir* **2018**, *34*, 1274.
[30] N. Sela, O. Ishai, *Composites* **1989**, *20*, 423.
[31] M. A. Isaacs, J. Davies-Jones, P. R. Davies, S. Guan, R. Lee, D. J. Morgan, R. Palgrave, *Mater. Chem. Front.* **2021**, *5*, 7931.
[32] S. Marcinko, A. Y. Fadeev, *Langmuir* **2004**, *20*, 2270.
[33] H. H. Kristoffersen, J. E. Shea, H. Metiu, *J. Phys. Chem. Lett.* **2015**, *6*, 2277.
[34] T. Loewenstein, A. Hastall, M. Mingebach, Y. Zimmermann, A. Neudeck, D. Schlettwein, *Phys. Chem. Chem. Phys.* **2008**, *10*, 1844.
[35] Y. Liu, K. Ai, L. Lu, *Chem. Rev.* **2014**, *114*, 5057.
[36] X. Du, L. Li, J. Li, C. Yang, N. Frenkel, A. Welle, S. Heissler, A. Nefedov, M. Grunze, P. A. Levkin, *Adv. Mater.* **2014**, *26*, 8029.
[37] M. L. Le, Y. Zhou, J. Byun, K. Kolozsvari, S. Xu, W. Chen, *Langmuir* **2019**, *35*, 12722.
[38] O. Carp, C. L. Huisman, A. Reller, *Prog. Solid State Chem.* **2004**, *32*, 33.
[39] P. Das, M. Reches, *Nanoscale* **2016**, *8*, 15309.
[40] J. Saiz-Poseu, J. Mancebo-Aracil, F. Nador, F. Busqué, D. Ruiz-Molina, *Angew. Chem., Int. Ed.* **2019**, *58*, 696.
[41] J. Liebscher, *European J. Org. Chem.* **2019**, *2019*, 4976.
[42] K. Lee, M. Park, K. G. Malollari, J. Shin, S. M. Winkler, Y. Zheng, J. H. Park, C. P. Grigoropoulos, P. B. Messersmith, *Nat. Commun.* **2020**, *11*, 5.
[43] H. Jiang, T. Zhao, C. Li, J. Ma, *Chem. Commun.* **2011**, *47*, 8590.
[44] M. B. Davidsen, J. F. L. Teixeira, J. Dehli, C. Karlsson, D. Kraft, P. P. C. Souza, M. Foss, *Colloids Surf., B* **2021**, *207*, 111972.
[45] V. Proks, J. Brus, O. Pop-Georgievski, E. Večerníková, W. Wisniewski, J. Kotek, M. Urbanová, F. Rypáček, *Macromol. Chem. Phys.* **2013**, *214*, 499.
[46] R. Luo, L. Tang, S. Zhong, Z. Yang, J. Wang, Y. Weng, Q. Tu, C. Jiang, N. Huang, *ACS Appl. Mater. Interfaces* **2013**, *5*, 1704.
[47] R. Luo, L. Tang, J. Wang, Y. Zhao, Q. Tu, Y. Weng, R. Shen, N. Huang, *Colloids Surf., B* **2013**, *106*, 66.
[48] D. Wu, X. Sun, X. Liu, L. Liu, R. Zhang, *Appl. Surf. Sci.* **2021**, *567*, 150813.
[49] M. Martín, A. G. Orive, P. Lorenzo-Luis, A. H. Creus, J. L. González-Mora, P. Salazar, *ChemPhysChem* **2014**, *15*, 3742.
[50] H. Li, Y. V. Aulin, L. Frazer, E. Borguet, R. Kakodkar, J. Feser, Y. Chen, K. An, D. A. Dikin, F. Ren, *ACS Appl. Mater. Interfaces* **2017**, *9*, 6655.
[51] H. Li, T. Marshall, Y. V. Aulin, A. C. Thenuwara, Y. Zhao, E. Borguet, D. R. Strongin, F. Ren, *J. Mater. Sci.* **2019**, *54*, 6393.
[52] K. G. Malollari, P. Delparastan, C. Sobek, S. J. Vachhani, T. D. Fink, R. H. Zha, P. B. Messersmith, *ACS Appl. Mater. Interfaces* **2019**, *11*, 43599.
[53] H. Li, J. Xi, Y. Zhao, F. Ren, *MRS Adv.* **2019**, *4*, 405.
[54] T. K. Slange, L. L. Warnet, W. J. B. Grouve, R. Akkerman, *Composites, Part A* **2018**, *113*, 189.
[55] Y. Su, M. de Rooij, W. Grouve, L. Warnet, *Composites, Part B* **2016**, *95*, 293.